Size distributions of submicron particles in oil and gas-fired residential boilers under variable combustion conditions. Correlation of Bacharach opacity index with soot mass concentration.

Santiago Jiménez*, Jorge Barroso, Antonio Pina, Javier Ballester

LIFTEC (CSIC-Universidad de Zaragoza), María de Luna, 10, 50018 Zaragoza, Spain

* Corresponding author. Phone: +34 976506520. Fax: +34 976506644. E-mail address: yago@litec.csic.es

Abstract

In spite of the relevance of residential heating burners in the global emission of soot particles to the atmosphere, relatively little information on their properties (concentration, size distribution) is available in the literature, and even less regarding the dependence of those properties on the operating conditions. Instead, the usual procedure to characterize those emissions is to measure the smoke opacity by several methods, among which the blackening of a paper after filtering a fixed amount of gas (Bacharach test) is predominant. In this work, the size distributions of the particles generated in the combustion of a variety of gaseous and liquid fuels in a laboratory facility equipped with commercial burners have been measured with a size classifier coupled to a particle counter in a broad range of operating conditions (air excesses), with simultaneous determination of the Bacharach index. The shape and evolution of the distribution with progressively smaller oxygen concentrations depends essentially on the state of the fuel: whereas the combustion of the gases results in monomodal distributions that 'shift' towards larger diameters, in the case of the gas-oils an ultrafine mode is always observed, and a secondary mode of coarse particle grows in relevance. In both cases, there is a strong, exponential correlation between the total mass concentration and the Bacharach opacity index, quite similar for both groups of fuels. The empirical expressions proposed may allow other researchers to at least estimate the emissions of numerous combustion facilities routinely characterized by their smoke opacities.

Keywords: Soot emission, residential boiler, Bacharach opacity index

1. Introduction

The opacity of flue gases from combustion facilities probably caused the first general concern about the atmospheric pollution, especially after the massive implementation of coal-fired boilers which accompanied the industrial revolution (Lestel, 2012). By the end of the nineteenth century this concern resulted in the development of the first techniques intended to, at least roughly, quantify the particulate emissions of industrial and domestic burners. Among them, the Ringelmann method, which compares the visual aspect of the smoke plume with a gray scale, became progressively popular and was adopted by researchers and institutions in Europe, first, and soon after also in the USA (Bureau of Mines, 1967; Lestel, 2012; Environmental Protection Agency (EPA)-method 9, 1907-2014). Ringelmann's smoke charts were a valuable way to monitor the concentration of particulates in flue gases, but the need for more quantitative methods motivated the proposal of new procedures, such as the smoke density test for distillate fuel burners (ASTM D2156, 1965), described below, gravimetric methods as the US EPA #5 (2014), or more recently the use of aerosol sizers and/or counters.

The method quoted in ASTM D2156 (or its equivalent DIN 51402) evaluates the "smoke density" of flue gases by filtering a fixed volume of these gases through a strip of standard filter paper and comparing the shade of the resulting spot with a reference gray scale, which due to the popularity of the instruments commercialized by Bacharach Inc. is also known as the Bacharach scale. The scale used to be divided in entire units from 0 to 9 for visual comparison with the spots, but the use of photometers allows for a greater resolution in recent models. According to the original ASTM text (1965), this method is much more sensitive to small concentrations of smoke than others available at that time; in particular, the entire Ringelmann scale (from 0 to 5) was said to correspond to spot number 9 (i.e. the maximum) in the 'new' method. The test was introduced around the mid-20th century (e.g. Bacharach Inc. registered the "true spot" trade mark in 1948) and soon became very popular among engineers and researchers in the field of liquid fuel combustion (for instance, it is referred to as the standard method in this industry in an EPA report due to Barrett et al. and dated 1973).

Most likely due to the complexity of the alternative techniques (as mentioned above, mainly gravimetric analysis or particle classifiers/counters) (Offen, 1976), definitely more precise and quantitative, the Bacharach scale and (even more strikingly) the Ringelmann charts are still mentioned as a reference in many regulations regarding domestic and also industrial burners. For instance, a certain value not to be exceeded in the startup or stationary functioning of a number of facilities is still quoted in the Spanish regulations (SPA, 1972; SPA, 2007a), as well as in other countries (e.g. CH, 1985; LUX, 1987; UK, 1993).

Incidentally, some of these regulations refer to the Bacharach scale also in relation with processes for which it was not designed or is directly inadequate, such as plants for the combustion of coal or other solid fuels, where the flue gases include not only soot but mainly fly-ash particles (SPA, 1972; SPA, 2007b). In spite of the progressive implementation of limits regarding mass and more recently number concentration of particulates in the emissions of stationary and mobile sources (e.g. in the European normative (EPC, 2009 and 2010), the lack of portable, affordable and easy-to-use instruments based on those techniques supports the pertinence of the traditional procedures, and in particular of the smoke density test, as a primary and routine check for the correct operation of several types of a variety of combustion facilities, especially domestic boilers.

There have been some attempts in the past to correlate the semi-empirical scales of Bacharach and Ringelmann with the mass concentrations actually present in the plumes considered. In principle, the dispersion of the sunlight in the plume, which is the basis of the Ringelmann's scale, can be theoretically reproduced by means of the Mie theory, if the particle size distribution and the corresponding refraction index are known (which is typically not the case, or not in detail). This was the approach followed by e.g. Pilat and Ensor (1970), who provided equations to estimate the mass concentration at a plume with a certain Ringelmann number. The introduction of transmissometers (or opacimeters) for measurements at the stacks reduced the uncertainties associated with the visual observations of the plumes, and thus a more reliable relation between light attenuation and mass concentration was expected; for instance, Conner and co-workers effectively reported roughly linear correlations of mass concentration vs. opacity, although the coefficients changed notably from plant to plant (and even with operating conditions in a plant), thus limiting the general application of any relationship (Conner, 1974; Conner and Knapp, 1988).

On the contrary, the authors are not aware of any attempt to theoretically correlate the Bacharach index with the aerosol mass concentration or, in other terms, the mass of the particles collected in the filter paper, which is probably due to the intrinsic complexity of the process of deposition on and within the paper and the subsequent light reflection on the surface. At the experimental side, only an EPA report (Barrett et al., 1974) has been found in which the potential correlation of the "Bacharach smoke number" and the particle mass concentration (measured according to EPA method #5) was specifically examined. The experiments were performed in two heating units with commercial fuel-oil #2, high pressure burners (~3.8 liters per hour) operated continuously or in cycles and with different levels of excess air. Most of the reported results corresponded to Bacharach indexes below 1, and none above 6 (which would have required a forcedly-bad combustion, probably). The cascade impactor used in their experiments to measure the size distribution couldn't actually distinguish between the different cases, with most of the mass below 0.25 μm (i.e. last plate of the impactor used). The authors concluded that a "practical" correlation between both measurements could be established for individual units under continuous operation (in practice, the series for the two units used fit well to the same correlation). Leary et al. (1987) investigated the composition of the material collected in filters (particles and organic 'extractables'), but only at two fixed Bacharach smoke numbers; as expected, the mass of particles increased with this parameter, but a precise trend was not derived. In a more recent work focused on the ability of different algorithms to correlate the Bacharach index and the operating parameters of a boiler, other researchers stated, however, that "there is no universal correlation between the Bacharach opacity of smoke and its mass content in solid particles as their size has a marked effect on the extent to which the filter paper [...] is blackened" (Blanco et al., 2000), although no reference is quoted for the statement. All in all, the impression of the authors of the present paper is that the Bacharach smoke test is routinely used in the fuel oil industry as the primary indicator not only of correct combustion, but also of particulate matter emission.

In the frame of several projects with oil and gas companies and recently with a research group interested in the fate of a fuel oil additive after combustion, a number of test series have been performed in the last two decades in one of LIFTEC's combustion facilities in which the Bacharach number was used in these ways. In some of these projects, the soot particles generated have been characterized, first by thermophoretic deposition on a TEM grid (and subsequent observation in a Transmission Electron Microscope) and, in the last years, also (or alternatively) by means of a particle classifier and counter. The latter provides detailed information on the particle number distribution and concentration in the gas sampled, and the total mass concentration can be derived from those data. The primary purpose of this paper is to present and discuss the data obtained in the simultaneous measurement of the Bacharach number and soot concentration in flue gases, in the seek of a practical correlation of both parameters (for the good of the former, popular and rather qualitative at present).

Besides, this article presents detailed particle size distributions (number and mass-weighed) corresponding to the emissions of two commercial burners for gaseous and liquid fuels for residential heating. The emissions of large combustion facilities under normal operation and those of vehicles have been well characterized in the past; on the contrary, not many works have been devoted to the domestic scale in spite of its practical relevance (for instance, fuel oil accounts for ~15% of the primary energy consumption in Spanish households (IDAE 2011), except for perhaps wood-fired facilities (e.g. Johansson et al., 2004), and none, to the authors' knowledge, has studied the dependence of the distribution on the operating conditions. The latter might be relevant for those interested in atmospheric aerosols and also provide information on the formation of soot aggregates in real flames.

2. Experimental methods, fuels and tests

The experiments have been carried out in a water-cooled chamber, schematically shown in Figure 1, intended to reproduce the conditions found in domestic boilers (up to 100 kW). The combustion chamber is cylindrical, with a length of 0.8 m, and is continued by a convergent section and a vertical tube, both also water-cooled. Finally, the gases flow along a horizontal tube towards a chimney. Two burners were used in the experiments reported in the present paper, in both cases commercial models: Kadet-Tronic 3R with a Danfoss 0.6 GPH, 60°S nozzle for fuel-oil, and Cuenod NC4 for gaseous fuels. In all the cases, the fuel consumption was regulated with the burner controls (at ~2.3 kg/h and ~0.8 Nm^3/h, respectively), and the air was supplied to the burner from a compressed air line fitted with a mass flow controller; in this way, a broad range of air/fuel ratios can be explored under a much more precise and stable regime compared to that attainable with the rather rough air regulation of the burners. The concentration of O_2, CO_2, CO and NO_x is monitored by sampling the flue gases at the horizontal tube. Under stable conditions, the oxygen concentration at the boiler outlet can be adjusted to within the resolution of the analyzer (0.1%).

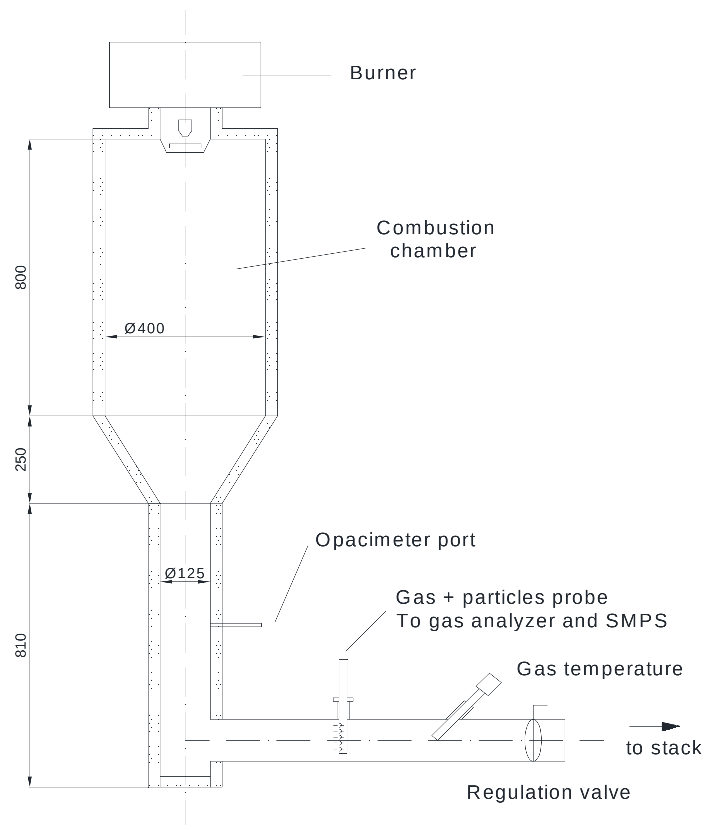

Fig. 1. Schematic view of the experimental facility. Dimensions in mm.

The smoke opacity test was applied at a sampling port located in the vertical tube. The instrument used, TESTO 308, extracts a fixed amount of gas at a constant rate and passes it through a strip of filter paper, whose blackening is subsequently determined by photometry with a precision of 0.1 in the Bacharach scale (0-9). Each test lasts about 60 seconds, except for the cases of very high Bacharach number (typically > 8.5), in which the instrument detects a high pressure drop at the paper, interrupts the test and extrapolates the result to its standard duration.

The measurement of the size and concentration of the particles in the flue gases required considerably greater effort. A secondary line was derived from the gas analyzer line and led to a silica-gel dryer; the temperature of the gas at the entrance of the latter was kept above 90°C to prevent water condensation. The resulting dry gas was re-sampled (36 l/h) by a scanning mobility particle sizer (SMPS, TSI 3936), composed of an aerosol classifier (TSI 3081) and a condensation particle counter (TSI 3782). The rest of the gases were filtered to protect the equipment downwards and passed through a mass flowmeter equipped with a valve to maintain ~400 Nl/h during the tests. The use of the silica dryer, as well as the tubes in the lines, causes a certain loss of particles, basically by diffusion, whose extent depends largely on their size. In order to evaluate these losses, a stable and broad distribution of NaCl particles was produced with an aerosol generator (TOPAS ATM 226 + dryer 570) and measured with and without the dryer and the tube from it to the entrance of the SMPS. The efficiency in the transfer through these elements is shown in Figure 2. As expected, the effect is very small for relatively large particles, and quite significant for the smallest: up to 50% of the 10 nm particles are lost. Due to the relatively complex geometry of the dryer (three mesh tubes surrounded by the silica beads, all inside a larger quartz tube) it is difficult to estimate these losses by calculation; nevertheless, a best fit of the data to the general equations for the deposition by diffusion in the case of a single tube (Baron and Willeke, 2001), also included in Fig. 2, shows the likely association of the losses to diffusion, and is thought to support the use of the correlation shown to correct the measurements. The SMPS software also takes into account the transport efficiency inside the instrument.

Two SMPS setups were required to cover the distribution of particles generated in the combustion facility, depending on the Bacharach index (also referred to as BI, hereafter), which resulted in two ranges of mobility equivalent diameters, 10-400 nm and 15-700 nm, with roughly 100 classes in both cases. SMPS measurements are given as number concentration of particles per volume of the carrying gas; the conversion to mass-weighed distributions will be commented later. Each mobility scan lasted two minutes; three independent results were averaged at each combustion condition. For BI above ~6, clogging of the five tiny inlets in the sampling probe (intended to collect a representative sample of the particles across the exhaust duct) was observed after some time and, to

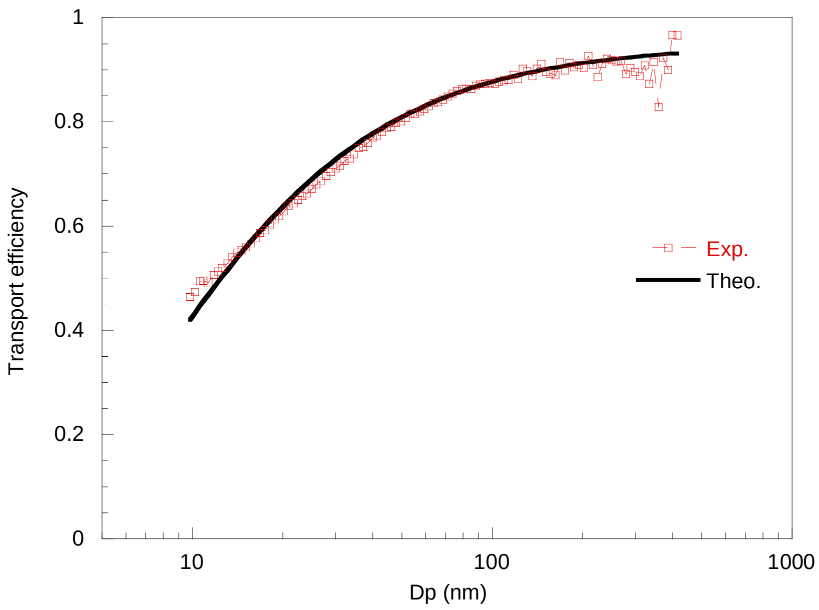

Fig. 2. Aerosol transport efficiency of dryer and tube. The theoretical curve corresponds to a best-fit to the general equation for losses due to diffusion in a tube (see text for details).

avoid artifacts in the results, the flow was inverted between measurements; during these 'cleaning events', the dryer line was closed to prevent dirtying and overpressure in the equipment.

The port used to perform the smoke opacity tests served also to collect particles by thermophoresis on a TEM grid covered with a carbon film for later observation and analysis in a 200 kV TEM. The grid was fixed to a 1x1x4 cm steel piece with two tiny drops of silver paint to ensure good thermal contact. A pneumatic cylinder inserted the piece into the hot gas stream during a controlled time, typically 30 s in high soot concentrations and 180 s in low opacity conditions; although the steel piece serves to slow down the grid's heating, longer times would result in significant deterioration of the film (for the same reason, Formvar films should be avoided). This system was used in the past for characterizing particle distributions through TEM image analysis; here, however, only a couple of images will be presented to illustrate the particles' morphology.

Data from two series of experiments will be reported, respectively focused on the use of butane/butene gaseous blends and on the fate of a Ce-based catalyst in the combustion of standard fuel-oil for domestic heating (No. 2 or C-type). In particular, five fuels were used: pure butane, a butane/butene blend (40/60%, respectively), pure fuel oil and the latter doped with 9 and 45 ppm of CeO_2, in the form of dispersed nanoparticles (Envirox, 8-10 nm according to the manufacturer). In all the cases, the controlled variable was the air-flow ratio by adjusting the air flow rate, regulated as explained above, for fixed fuel consumption; this resulted in different gaseous and particulate concentrations in the flue gases, which in this work will be characterized by the corresponding BI's (closely related to the oxygen concentration in flue gases or, in other words, the air excess).

3. Results

Figures 3 to 6 present the size distributions (number weighed) of the particles generated in the combustion of butane, butane/butane, fuel oil and fuel oil doped with 9 ppm of CeO_2, respectively, in combustion conditions such that the Bacharach covers the range 0.3-8.5; the results for the fuel oil doped with 45 ppm CeO_2 do not differ significantly from those for 9 ppm, and are omitted in these figures. The data are expressed as measured at the SMPS, i.e. dry gases at room conditions (~20°C, 1 atm). The corresponding number-based mean diameters and total particle concentrations are shown in Figure 7. There is an evident similarity among the distributions generated in the combustion of the gaseous and the liquid fuels, respectively, and clear differences between both groups. Firstly, in the case of the butane and butane/butene flames, the total number of particles increases slightly with BI for very low BI's, and then remains essentially constant except for the highest BI's, where it decreases; on the contrary, the distributions corresponding to the liquid fuels show a consistent decrease of the total number of particles for increasing Bacharach indices. Secondly, the distributions for the gaseous fuels are always monomodal and mostly 'shift' towards larger diameters with BI, whereas a more progressive broadening of the distributions is observed in the case of the liquid fuels, with a trend towards a bimodal distribution that will be more clearly noticed in the mass weighed representation shown later; larger mean diameters (in number) are observed for the gases than for the fuel oils. Finally, in conditions which result in very low smoke opacity numbers (BI < 1) the size distribution of the gaseous fuels has a long tail towards big diameters (up to ~100 nm) and relatively few particles in the lower limit of the SMPS (~10 nm here), while for the fuel oils a significant fraction of the particles seems to be actually below this limit and a much shorter tail is observed (up to 30-40 nm). Note also that in these conditions the number of particles generated in the combustion of fuel oils is nearly one order of magnitude greater than when the gases are burnt. In the authors' opinion, these differences may be attributed to the different ways in which soot is formed in each case: mostly locally, in the vicinity of the fuel droplets, or more extendedly, in regions where the appropriate conditions are found, for the gases.

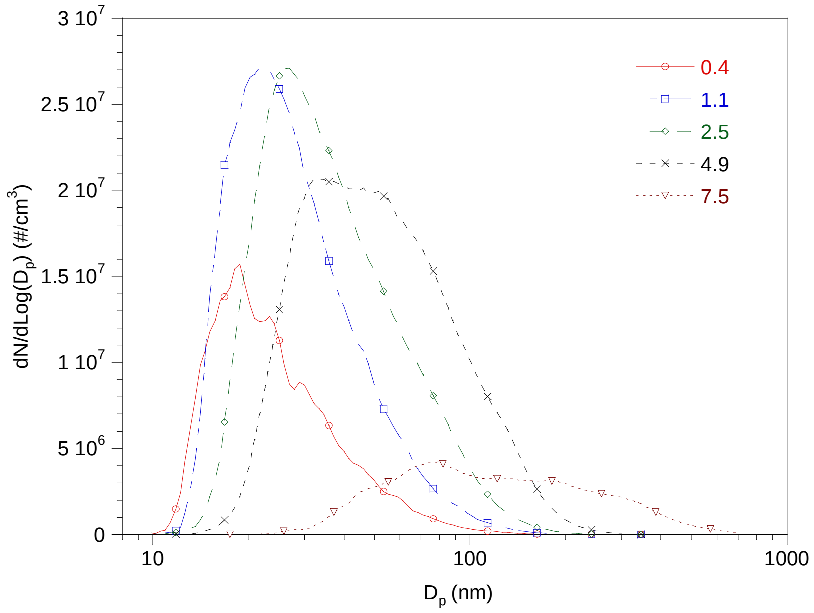

Fig. 3. Number-weighed particle size distribution of the particles generated in the combustion of butane. The numbers in the legend indicate the corresponding Bacharach opacity index. dLogDp ≈ 0.0156 for all the measurements shown in this work. Y-units refer to dry gases at standard room conditions (~20°C, 1 atm), which applies also to the rest of the figures.

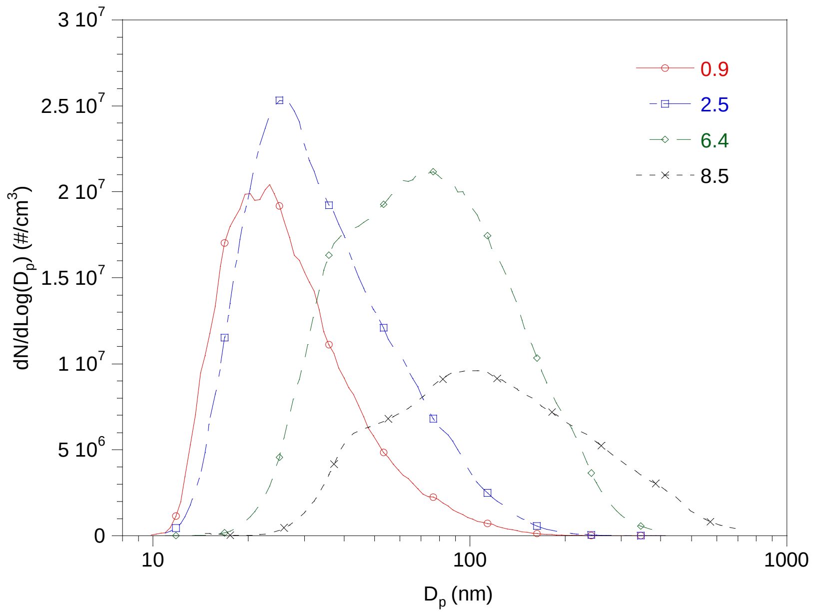

Fig. 4. Number-weighed particle size distribution of the particles generated in the combustion of a butane/butene blend.

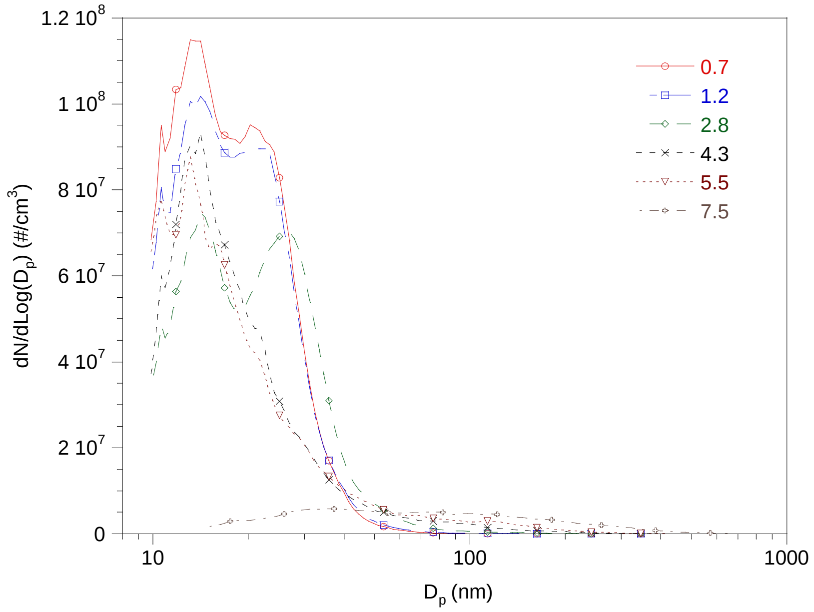

Fig. 5. Number-weighed particle size distribution of the particles generated in the combustion of fuel oil.

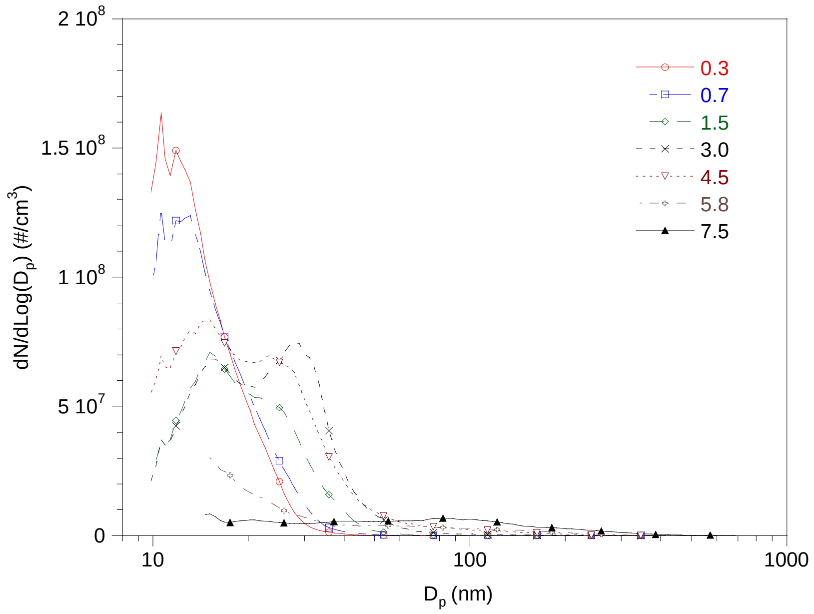

Fig. 6. Number-weighed particle size distribution of the particles generated in the combustion of fuel oil doped with 9 ppm CeO_2.

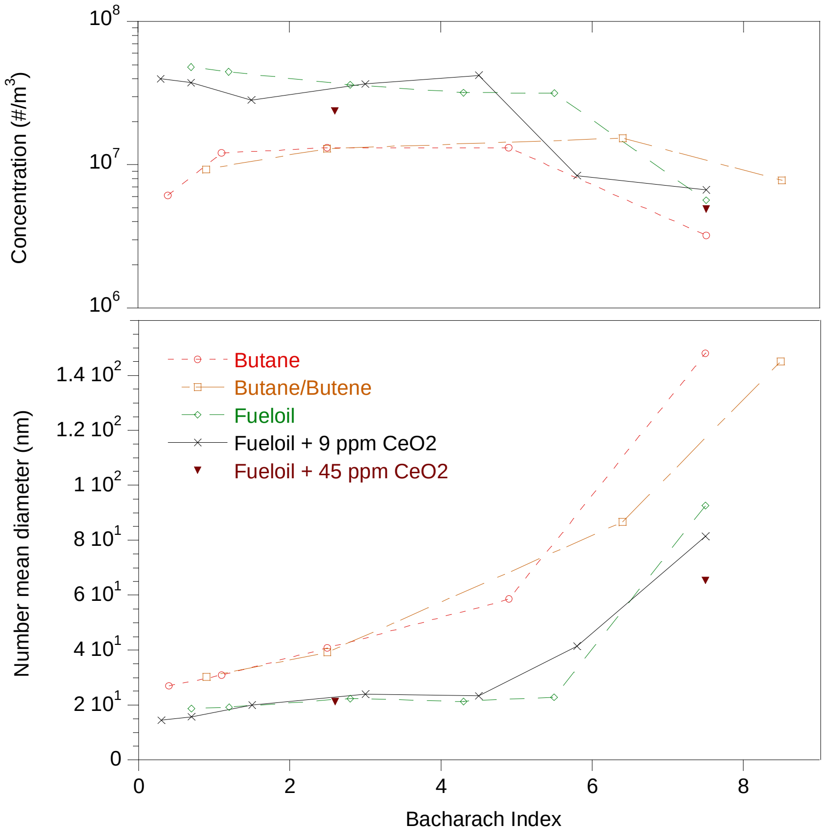

Fig. 7. Mean particle diameter (in number, bottom) and total number concentration (top) as a function of the Bacharach index for the fuels considered in this work.

Specifically regarding the fuel oils, the CeO_2 nanoparticles dispersed in some tests might explain the presence of a very high number of ultrafine (10-20 nm) particles in nearly non-sooting conditions (BI → 0), which is not observed in fuel-oil tests without additive. This association must be made with caution, though, since the particles have not been analyzed in this study. In the past, isolated particles solely composed of iron could be identified in the smoke generated in the combustion, in this facility and under similar conditions, of fuel oils with other additives.

In principle, the mass weighed particle distributions should be readily derived from the number based ones, already commented, by simply considering the volume and the density of the particles. Nevertheless, this has proven not to be a straightforward process. The diameter used in the previous figures (and in those below) refers to the mobility equivalent diameter, i.e. that of a sphere with the same electrical mobility than the measured particle. The use of this diameter to estimate the volume of the particle is thus a first (common) approximation. The determination of the particle's density is however more complex and, as pointed out previously by Maricq and Xu (2004), represents the main difficulty in the application of this kind of particle counting methods to measurements of aerosol mass concentration. Figure 8 shows the typical aspect of the particles

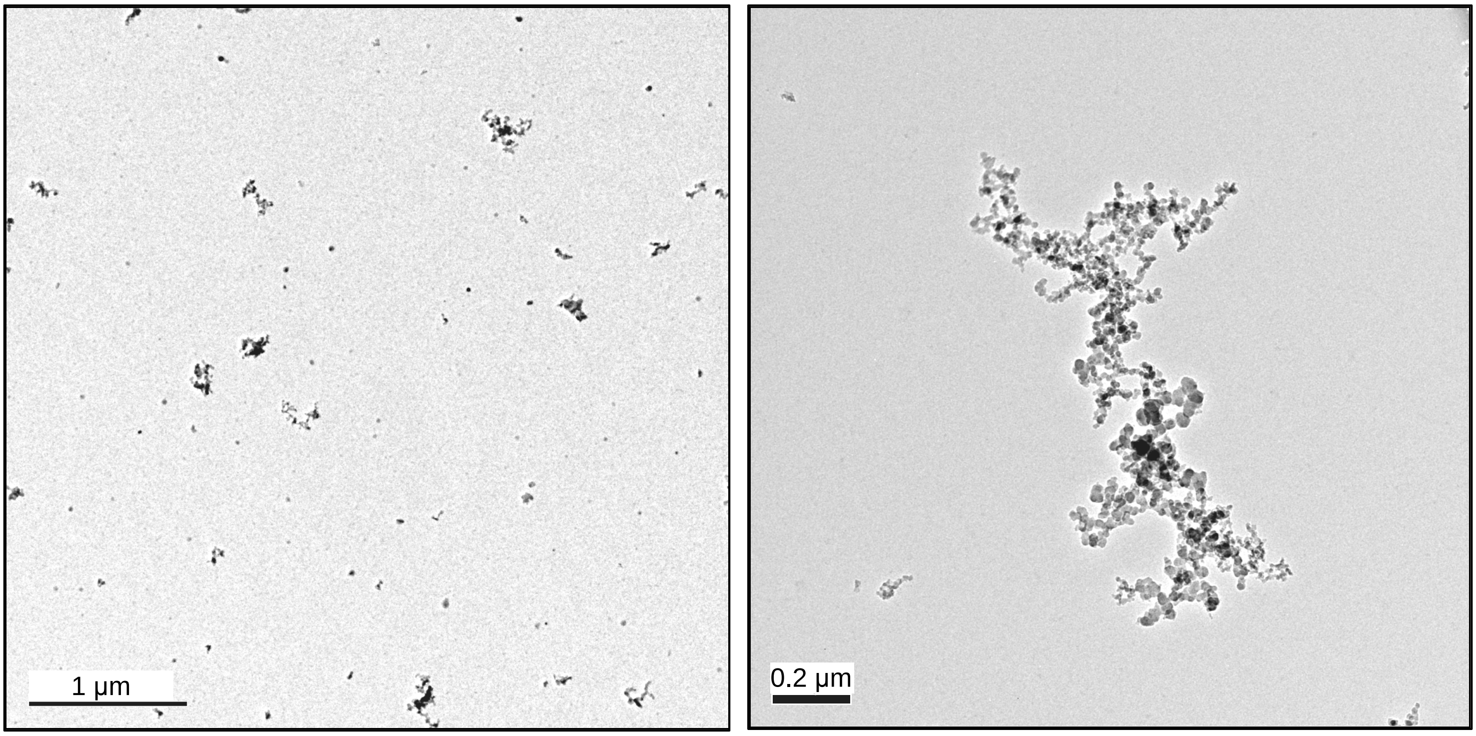

Figure 8. TEM images of soot particles collected in prior tests with fuel oils. Bacharach indices ~3 (left) and ~9 (right). Typical distribution and aspect of a large aggregate, respectively.

collected on TEM grids by thermophoresis in tests with fuel oils in a prior study, and are intended to illustrate the evolution of the particles' morphology with their size. Whereas the smallest particles are composed of a single or few ultrafine (10-20 nm) corpuscles forming a relatively compact, nearly spherical body, an increase in size is basically the consequence of the aggregation of a greater number of those corpuscles. The fractal-like nature of these large aggregates is at present well stated (e.g. Friedlander, 2000); based on this, an expression for the dependence of their effective density on their diameter can be derived:

$$\rho_{eff} \sim D_p^{D_f-3} \quad (1)$$

where D_f is the fractal dimension of the aggregate. For soot, this parameter takes a value around 2.2 (e.g. Sorensen, 2011), so that an increase in size implies a decrease in effective density. The expression is valid only for aggregates containing a high number of corpuscles, and obviously not for isolated corpuscles or accumulations of few of them, for which an effective density similar to the intrinsic density of the material (~ graphite, in this case) is expected. Some works in the last decade have reported direct measurements of the particles' densities, in setups where the mass of particles within a narrow mobility (selected by a DMA) was determined with another instrument (impactor, aerodynamic aerosol classifier, etc). Figure 9 shows the densities of soot aggregates generated in various combustion systems, from a candle

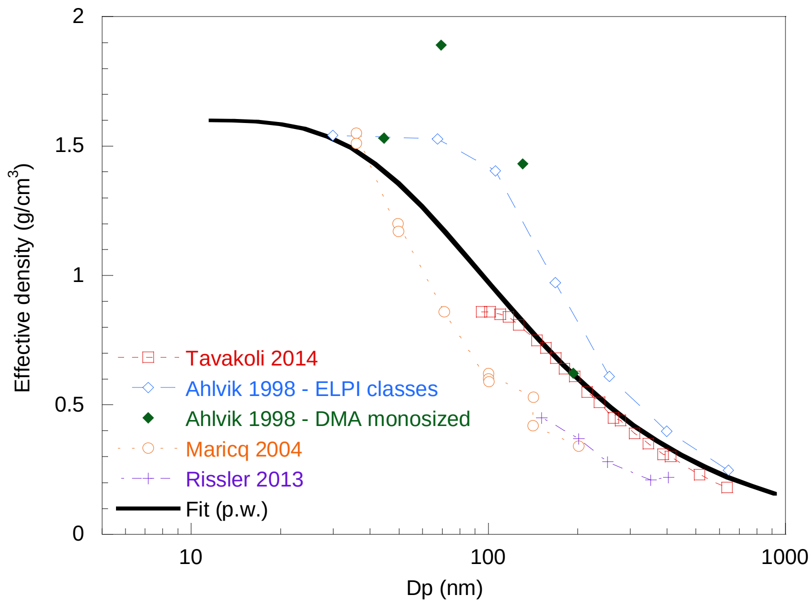

Fig. 9. Effective soot density as a function of mobility diameter. See text for details.

(Rissler et al., 2013) to diesel vehicles (Ahlvik et al., 1998) or methane (Tavakoli and Olfert, 2014) and ethylene (Maricq and Xu, 2004) burners, determined in that way. All the series reflect a decrease in density with particle diameter that is well fitted by eq. (1) with $D_f \sim 2.2$, which evidences the need for taking this effect into account in the derivation of the mass distributions from the number-weighed ones. Unfortunately, the size at which the curves start to decay varies notably within the measurements reported and the reason for the difference is unclear; a reasonable fit of the ensemble of experimental data shown in Fig. DD, also plotted in this graph, that approaches eq. (1) asymptotically is obtained with the following expression:

$$\rho_{eff} = \rho_b \left(1 - Exp\left(\frac{D_a}{D_p}\right)\right) + \rho_b \left(-Exp\left(\frac{D_a}{D_p}\right)\right) D_p^{\,D_f - 3} \qquad (2)$$

with D_a = 90 nm, D_f = 2.2 and ρ_b = 1.6 g/cm^3. The value of D_a was chosen to fit the available data; qualitatively, it represents the size of the (still small) aggregate that contains a number of corpuscles sufficient to notably decrease its effective density with respect to that of the corpuscles (ratio ~0.6 here). Eq. (2) might be of course adapted to other corpuscles' sizes by simply changing the value of this parameter.

Figures 10 to 13 present the mass-weighed distributions derived from the original number-based ones through application of the correlation 2 for the particle density. As in the previous representation, the gaseous and the liquid fuels can be grouped separately, with minor differences within each group. In the combustion of butane and butane/butene, a single, broad mode of particles

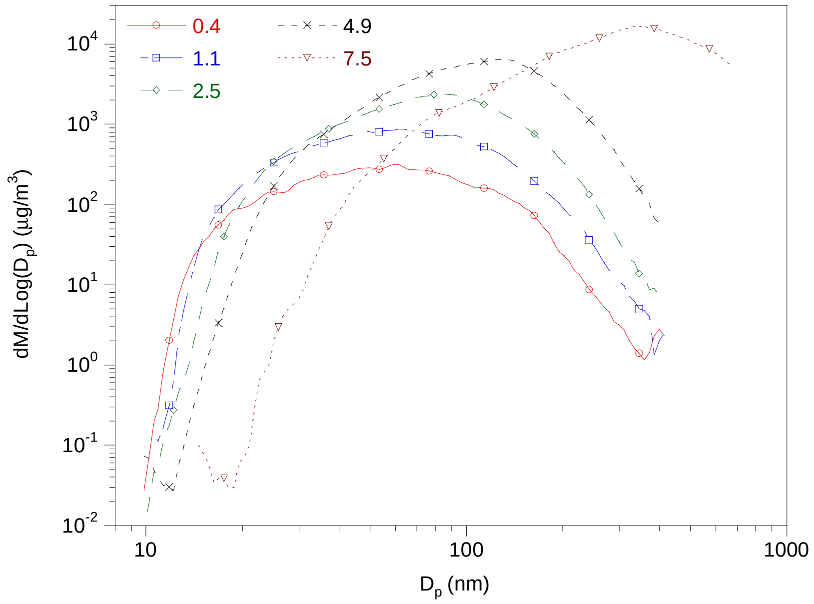

Fig. 10. Mass-weighed particle size distribution of the particles generated in the combustion of butane.

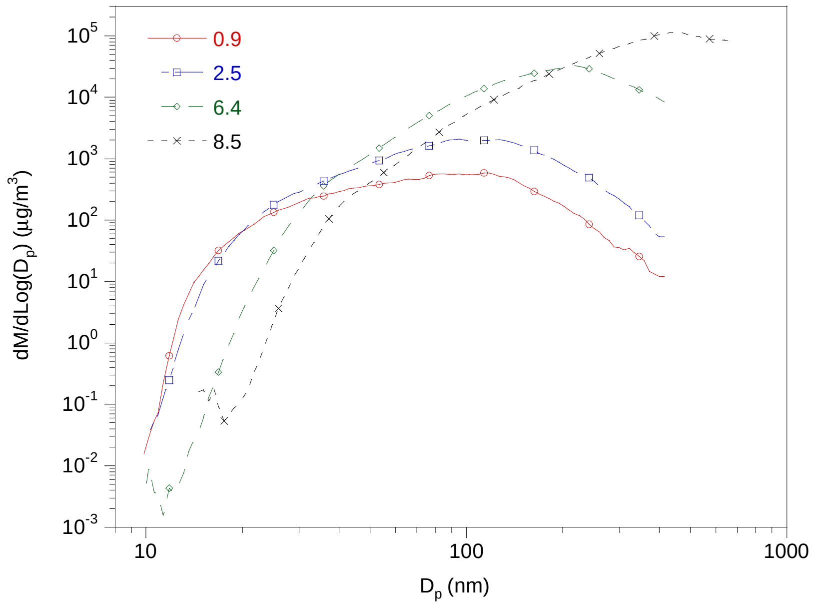

Fig. 11. Mass-weighed particle size distribution of the particles generated in the combustion of a butane/butene blend.

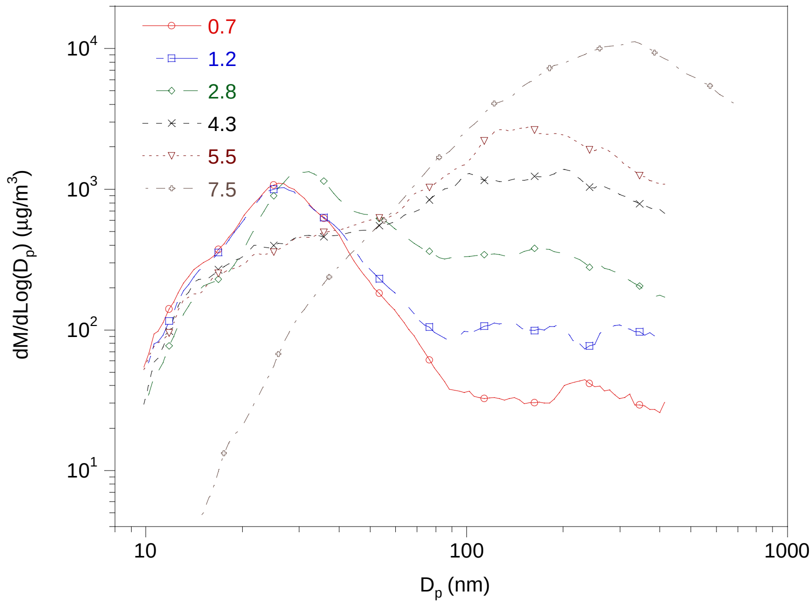

Fig. 12. Mass-weighed particle size distribution of the particles generated in the combustion of fuel oil.

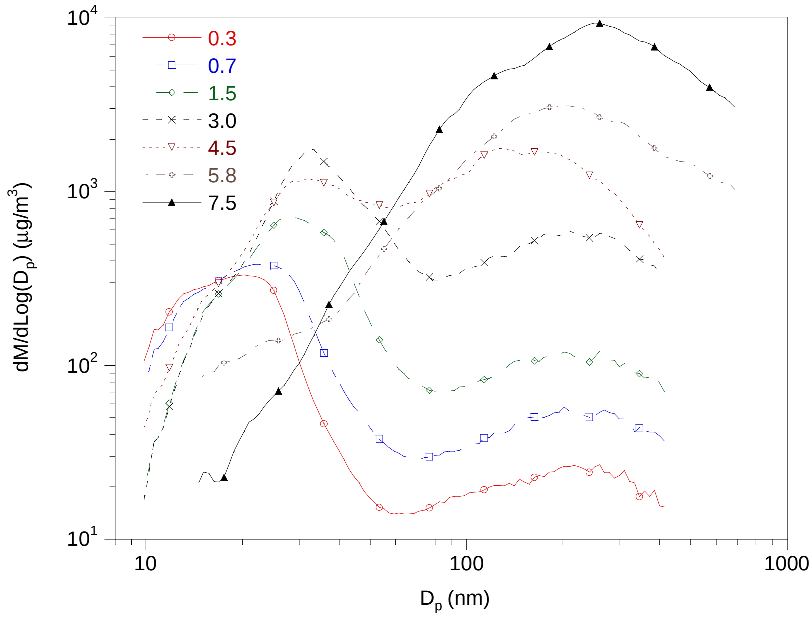

Fig. 13. Mass-weighed particle size distribution of the particles generated in the combustion of fuel oil doped with 9 ppm CeO2.

is observed, increasingly shifted towards greater sizes and mass concentrations for increasing Bacharach indices (~lower oxygen concentrations). In the case of the fuel oils, a bimodal distribution is generally found, with a fine mode (<100 nm) that grows both in concentration and mean size until BI~3 and then is rapidly absorbed by the 'coarse' particle mode, whose relative and absolute importance increases very markedly with the Bacharach index; at high BI's this

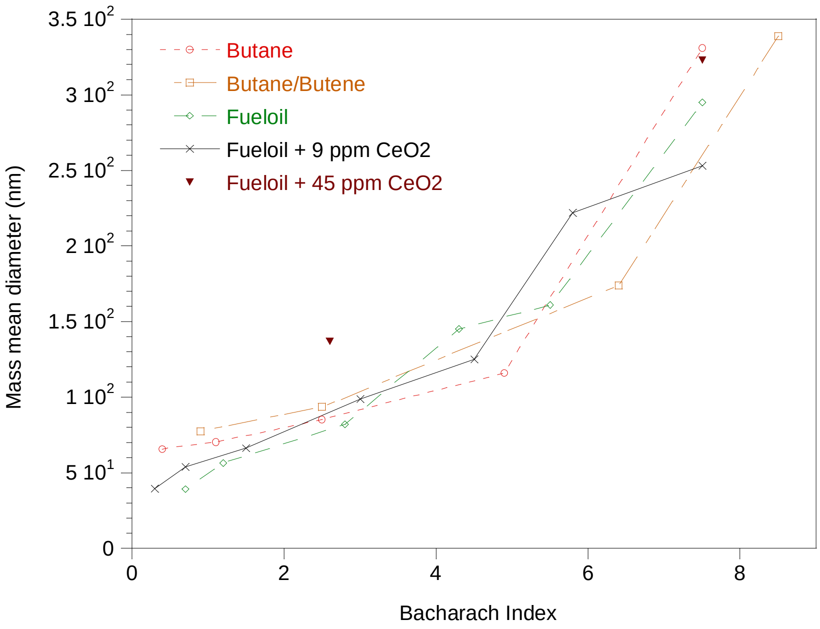

Fig. 14. Mean diameter (mass weighed) vs. Bacharach index.

latter mode is the only one observed. As commented above, these differences between fuels are most likely associated to a different occurrence of the conditions where the soot is formed. At high BI's all the fuels generate a similar monomodal distribution, however, probably reflecting the dominance of coagulation in such particle-saturated conditions.

The mean particle diameter in mass, shown in Figure 14, increases with BI, as expected, and basically coincides for all the fuels at the same Bacharach index. As just commented, this coincidence does not reflect a uniform shape or behavior of the size distributions. Finally, Figure 15 presents the dependence of the total mass concentration on the Bacharach index. The concentrations span nearly two orders of magnitude for each fuel in the range of BI 0.3-8.5, with roughly a factor of two between the data corresponding to the gaseous fuels and those of the fuel oils for the same BI. There is a clear dependence of the total aerosol concentration on this parameter (and vice versa), very similar in trend for all fuels in spite of the differences found in the size distributions presented above, especially regarding both types of fuels. A practical correlation found as a fit of all the data included in Fig. 15 is

$$C\,[\mu g/sm^3] = 220\, e^{0.47\,BI} \qquad (3)$$

where C is the total aerosol concentration (at room or 'standard' conditions). A more specific correlation for each class of fuels is obtained by multiplying the former expression by ~1.4 and 0.7 for gaseous and liquid fuels, respectively, and keeping the exponent.

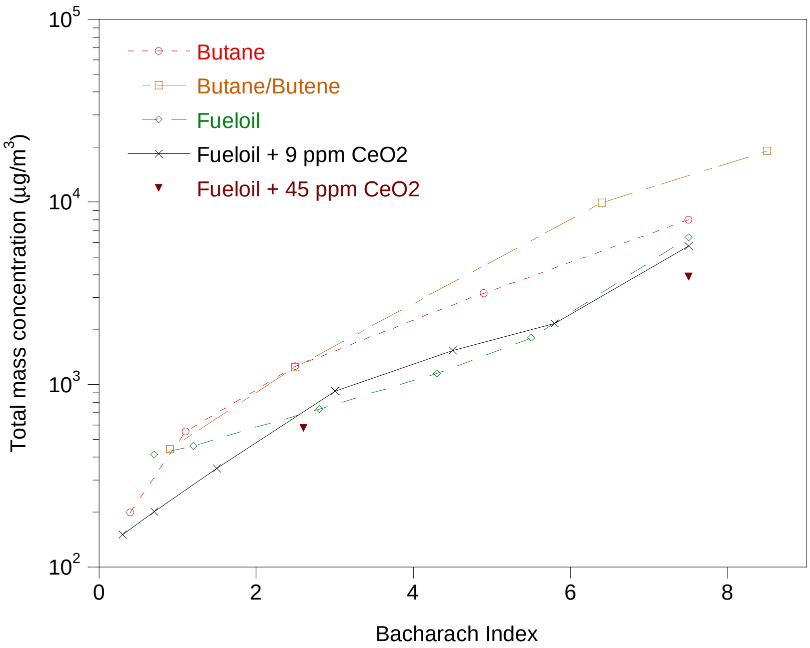

Fig. 15. Aerosol mass concentration vs. Bacharach opacity index for all the fuels studied.

The uncertainty in the effective density of the aggregates, previously discussed, would affect the absolute values in this C vs. BI correlation, but not the existence of the exponential correlation and the uniformity of the exponent among fuels (~0.6). For instance, assuming a uniform ρ_{eff} = 1.6 g/cm^3, the concentration would have been ~3.5 times higher than that plotted in Fig. 15 for the highest BI (minor changes for the lowest), with an exponent ~0.6 instead of 0.47; as shown in Fig. DD, this assumption would be actually quite unrealistic, and is commented here only to support the exponential correlation and also indicate a (highly over-) estimate for its uncertainty at the highest BI's.

Barrett et al. (1974) reported also an exponential relation between particulate loading (determined following US EPA method #5) and Bacharach smoke number in fuel oil fired boilers, with a similar exponent but nearly one order of magnitude above the concentrations presented in Fig. 15. Most of their data corresponded to BI<1, with a dispersion comparable to the reported mean values. The authors did not comment on the properties of the matter collected in the filters; in a later work, Leary et al. (1987) investigated the composition of material collected in a similar way in a facility equipped with a residential oil burner and found it included a significant fraction of compounds soluble in organic solvents, especially in low BI conditions, which was attributed both to sampling artifacts and to unburnt fuel. Whereas this may reduce the actual concentrations reported by Barrett and co-workers by a factor of up to two, it wouldn't make their data to agree quantitatively with those presented here. Leary et al. reported average values of 6 and 55 mg of particulates per kg of fuel fired for BI equal to 1 and 5 in continuous operation, respectively, which once re-expressed in terms of mass per standard volume of dry flue gases (correspondingly ~15-12 sm3/kg of fuel) agree fairly well with the data quoted in Fig. 15. This agreement, and the fact that Leary and co-workers used a different facility equipped with an unmodified commercial burner (which according to their report showed some temporal instabilities), is thought to further support the generality and thus practicality of the empirical correlation given above.

4. Conclusions

The size and concentration of soot particles generated in the combustion of several gaseous and liquid fuels in a residential heating burner has been measured in a broad range of operating conditions (oxygen excess values) by means of a particle classifier coupled with an optical counter. Those measurements have been complemented with routine smoke opacity tests, with results expressed in the commonly used Bacharach opacity scale.

The directly measured, number-weighed particle size distributions show a distinct behaviour for the gaseous and liquid fuels, respectively. Whereas for the former fuels the distribution 'shifts' towards larger diameters with lower oxygen excess values - higher Bacharach indices, in the case of the liquid fuels a progressive broadening of the distribution is observed. In both cases, the mean particle diameter increases with BI, through the formation of progressively bigger aggregates, and the total number of particles shows a mild dependence on that index.

In order to derive the corresponding mass-weighed distributions, a correlation for the dependence of the aggregate density on their size has been proposed, based on the experimental data available in the literature for supposedly similar soot particles and also on theoretical, asymptotical considerations for isolated corpuscles and big aggregates. The mass distributions may again be grouped according to the type of fuel, with little (if any) differences within each group: in the case of the gaseous fuels, a monomodal distribution moves toward larger diameters, whereas in that of the gas-oils the mass distribution is clearly bimodal and the mode in larger diameters progressively grows in relevance for lower oxygen concentrations in flue gases. The mean mass-weighed diameter is however similar for all the fuels and, as expected, increases steadily with BI. There is a strong exponential correlation between the total mass concentration and the Bacharach index, given by eq. 3 above for the set of all fuels, which may be refined for the liquid and gaseous fuels separately.

The data provided in this work reasonably agree with the scarce ones reported by other researchers in the past; in the authors' opinion, this fact supports the reliability of the correlations proposed, which in the end constitute a way to roughly estimate soot mass concentrations from the opacity tests routinely made in residential heating units.

Acknowledgements

The authors acknowledge the help of L. Ojeda and A. Campos with the experimental tasks.

References

Ahlvik, P., Ntziachristos, L., Keskinen, J. and Virtanen, A. Real time measurements of diesel particle size distribution with an electrical low pressure impactor, SAE Technical paper series 980410 (1998).

ASTM. D2156: Method of tests for smoke density in flue gases from distillate fuels. 1965, re-approved in several occasions (last 2013).

Baron, P.A. and Willeke, K. (eds.), Aerosol Measurement. Principles, techniques and applications, 2nd edition, Wiley & Sons, 2001.

Barrett, R.E., Miller, S.E. and Locklin, D.W. Field investigation of emissions from combustion equipment for space heating. Environmental protection agency report, EPA-R2-73-084a, 1973. Available at e.g. nepis.epa.gov.

Barrett, R.E., Locklin, D.W. and Miller, S.E. Investigation of particulate emissions from oil-fired residential heating units. Environmental protection agency report, EPA-650/2-74-026, 1974. Available at e.g. nepis.epa.gov.

Blanco, M., Coello, J., Maspoch, S., Puigdomènech, A., Peralta, X., González, J.M. and Torres, J. Correlating Bacharach opacity in fuel oil exhaust. Prediction of the operating parameters that reduce it, Oil and Gas Science and Technology - Rev. IFP, 55:5, 533-541, 2000.

Bureau of Mines, 1967. Ringelmann Smoke Chart, Information Circular 8333, Bureau of Mines, US Department of Interior, 1967.

CH, 1985. Conseil fédéral suisse, Ordonnance sur la protection de l'air (OPair), 1985. www.admin.ch (In French, German, Italian and English (non-official translation)).

Conner, W.D. Measurement of the opacity and mass concentration of particulate emissions by transmissometry, Environmental protection agency report, EPA-650/2-74-128, 1974. Available at e.g. nepis.epa.gov.

Conner, W.D. and Knapp, K.T. Relationship between the mass concentration and light attenuation of particulate emissions from coal-fired power plants, JAPCA 38:2, 152-157, 1988.

Environmental Protection Agency (USA). Method 5: Determination of particulate matter emissions from stationary sources, Code of Federal Regulations, 40-I-C-Part 60-Appendix A, current as 2014, www.ecfr.gov .

Environmental Protection Agency (USA). Method 9: Visual Determination of the Opacity of Emissions From Stationary Sources, Code of Federal Regulations, 40-I-C-Part 60-Appendix A, 1907, current as 2014, www.ecfr.gov .

EPC, 2009. European Parliament and Council, Regulation 595/2009. 2009.

EPC, 2010. European Parliament and Council, Directive 2010/75/EU on industrial emissions. 2010.

Friedlander, S. K., Smoke, dust and haze. Fundamentals of aerosol dynamics, Oxford University Press, NY, 2000.

IDAE, 2011. IDAE (Spanish Ministry of Industry, Commerce and Tourism). SECH-SPAHOUSEC. Analysis of the energy consumption in the Spanish households. Final Report. 2011. http://www.idae.es (In Spanish).

Johansson, L.S., Leckner, B., Gustavsson, L., Cooper, D., Tullin, C. and Potter, A. Emission characteristic of modern and old-type residential boilers fired with wood logs and wood pellets, Atmospheric Environment, 38, 4183-4195 (2004).

Leary, J.A., Biemann, K, Lafleur, A.L., Kruzel, E.L., Prado, G.P., Longwell, J.P. and Peters, W.A. Chemical and toxicological characterization of residential oil burner emissions: 1. Yields and chemical characterization of extractables from combustion of no. 2 fuel oil at different Bacharach smoke numbers and firing cycles, Environmental Health Perspectives, 73, 223-234 (1987).

Lestel, L. Pollution atmosphérique en milieu urbain: de sa régulation à sa surveillance, *VertigO - la revue électronique en sciences de l'environnement*, Hors-série 15 | février 2013. URL: http://vertigo.revues.org/12826; DOI: 10.4000/vertigo.12826

LU1987, Règlement grand-ducal modifié du 23 décembre 1987 relatif aux installations de combustion alimentées en combustible liquide, re-approved in 2008. http://www.legilux.public.lu (in French).

Maricq, M. M. and Xu, N. The effective density and fractal dimension of soot particles from premixed flames and motor vehicle exhaust, Aerosol Science and Technology, 35, 1251-1274 (2004).

Offen, G.R., Kesselring, J.P., Lee, K., Poe, G. and Wolfe, K.J. Control of particulate matter from oil burners and boilers. Environmental protection agency report, EPA-450/3-76-005, 1976. Available at e.g. nepis.epa.gov.

Rissler, J., Messing, M.E., Malik, A.I., Nilsson, P.T., Nordin, E.Z., Bohgard, M., Sanati, M. and Pagels, J. Effective density characterization of soot agglomerates from various sources and comparison to aggregation theory, Aerosol Science and Technology, 47:7, 792-805 (2013).

Sorensen, C.M. The mobility of fractal aggregates: a review, Aerosol Science and Technology, 45:7, 765-779 (2011).

SPA, 1972. Law 38/1972, December 22nd, on the Protection of the Atmospheric Environment, and subsequent revisions. www.boe.es (In Spanish).

SPA, 2007a. Real Decreto 1027/2007, Reglamento de Instalaciones Térmicas en Edificios, www.boe.es (In Spanish).

SPA, 2007b. Spanish Ministry of Industry, Commerce and Tourism. Guía técnica sobre procedimiento de inspección periódica de eficiencia energética para calderas, 2007 (in Spanish).

Tavakoli, F. and Olfert, J.S. Determination of particle mass, effective density, mass-mobility exponent, and dynamic shape factor using an aerodynamic aerosol classifier and a differential mobility analyzer in tandem, Journal of Aerosol Science, 75, 35-42 (2014).

UK1993. UK Clean Air Act 1993. http://www.legislation.gov.uk.